NATIONAL AIR INTELLIGENCE CENTER

ELECTRO-OPTIC EFFECT IN THE PESO
ACOUSTO-OPTIC MODULATOR

by

Tai Renzhong, Lu Futun, et al.

DTIC
ELECTE
NOV. 17, 1994
S B D

94 1116 040

94-35385

DTIC QUALITY INSPECTED 5

HUMAN TRANSLATION

NAIC-ID(RS)T-0395-94   9 November 1994

MICROFICHE NR: 94C000467

ELECTRO-OPTIC EFFECT IN THE PESO
ACOUSTO-OPTIC MODULATOR

By: Tai Renzhong, Lu Futun, et al.

English pages: 11

Source: Wuli Xuebao, Vol. 41, Nr. 6, June 1992,
pp. 1012-1018

Country of origin: China
Translated by: Leo Kanner Associates
F33657-88-D-2188
Quality Control: Nancy L. Burns
Requester: NAIC/TATA/J.M. Finley
Approved for public release; Distribution unlimited.

GRAPHICS DISCLAIMER

All figures, graphics, tables, equations, etc. merged into this
translation were extracted from the best quality copy available.

ELECTRO-OPTIC EFFECT IN THE PESO ACOUSTO-OPTIC MODULATOR

Tai Renzhong, Lu Futun, Yuan Shuzhong, Guan Xin'an, and Li Bing;
all of Institute of Modern Optics, Nankai University, Tianjin
30071

ABSTRACT

With the theory of one-dimensional approximation, combined with the boundary condi-
tions, an inhomogeneous electric field is derived from the foundamental equations of pieozoelec-
tric effect. This inhomogeneous electric field will lead to generation of "electric grating", and
"high-order grating" can also appear owing to coupling between "electric grating" and "acous-
tic grating". Linear electro-optic effect in PESO modulator is helpful to the diffraction and
modulation of the incident light beam. The experimental results verify our conclusions.

I. Introductory

The diffraction efficiency and modulation depth of the PESO
stationary wave type acousto-optic modulator are very high. Turi
et al [1] analyzed the angle of energy production; they
discovered that this modulator, which integrates transducer and
acousto-optic interaction. can utilize electric power supply at
high efficiency. In other words. the effective electro-acoustic
transformation efficiency is very high, thus promoting a higher
modulation percentage. In this case. consideration is given only
to the acoustic grating, not to the effect of electric field.
Meanwhile, when Turi et al determined the optimal diffraction
orientations of LiNbO$_3$ crystal $\Delta n_1/\Delta n_{30}, \Delta n_2/\Delta n_{30},$ and

$\Delta n_{31}/\Delta n_{m}$ are theta=30° and theta=90°. Along these two orientations, the electro-optic effect is restricted to the maximum extent $(\Delta n_{31} = \Delta n_1 - \Delta n_1$ and $\Delta n_{m} = \Delta n_1' - \Delta n_1$; Δn_i and $\Delta n_i' (i=1,2)$ are variations of acousto-caused and electro-caused refractivity of the principal axis). However, as research showed, this electro-optic effect of $Y_0 o$ or $Y_{30} o$ in a piezoelectric crystal is not a disadvantageous factor. The constant of the acousto-optic grating produced by a piezoelectric-induced acoustic stationary wave is identical to the constant of the primary grating caused by the inhomogeneous distribution of electric field. Both constants have a positive promoting function to diffraction and modulation of an incident light beam.

II. Theoretical Analysis

In the rectangular piezoelectric resonator as shown in Fig. 1, there are quite a few intrinsic sound modes [2]. When the external driving frequency is the intrinsic frequency, an intrinsic mode will be set in oscillation. Generally, it is very complex to precisely solve for these intrinsic modes. Thus, for convenience in analysis, the one-dimensional approximation theory [3] of Ristic thin sheet resonator is adopted. In order to adapt this theory to $LiNbO_3$ crystal of $Y_1 o$, the following assumptions are made (all these assumptions were experimentally validated).

1) crystal width w is greater than the crystal thickness d (in experiments, $w \sim 3d$);
2) squeezing along the x-direction, eliminate the x polarized shear wave (S. wave); and
3) squeezing along the z direction for nonilluminated portion, reduce as much as possible the z polarized shear wave (S. wave).
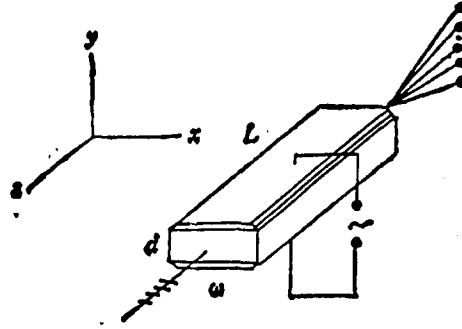
Fig. 1. Schematic Diagram
of Piezoelectric Resonator
(Mg-doped LiNbO, crystal)
x, y and z axes and X, Y
and Z crystal axes

At the same time, Turi's investigation further indicated
that the attenuation of shear wave is much greater than the
attenuation of the longitudinal-direction wave. Therefore, at
the steady state, the main effect on diffraction of the incident
light beam is caused by the acoustic longitudinal wave.

Based on the foregoing conditions, the y-axis can be
approximately considered as the direction of the pure-mode axis;
thus, the one-dimensional approximation can be adopted. In other
words, all the various related field quantities are functions of
coordinate y and time t. Thus, the equations of piezoelectric
characteristics can be simplified as follows:

$$T_2 = C_{11}^E S_2 - e_{22} E_2,$$ (1)

$$D_2 = e_{22} S_2 + s_{11}^e E_2,$$ (2)

In the equations, T_2 is stress; E_2, D_2 are, respectively, vectors
of electric field and electric charge displacement. C_{11}^E is the
coefficient of elasticity of the medium in the absence of an
electric field. s_{11}^e is the dielectric coefficient of the medium
in the absence of deformation; e_{22} is the piezoelectric
coefficient. Strain S_2 can be expressed as

$$S_2 = \frac{\partial u_2}{\partial y},$$ (3)

In the equation, u_2 is the magnitude of translation of particles

3

(in the medium) along the y axis. Newton's Second Law in a continuous medium is

$$\partial T_1/\partial y = \rho m \partial^2 u_1/\partial t^2, \qquad (4)$$

In the equation. ρ_s is the density of the medium. In the quasi-electric field approximation, the electric field E_2 can be expressed as

$$E_2 = -\frac{\partial \varphi}{\partial y}, \qquad (5)$$

Phi is the distribution of electric potential in the medium. The movement equation of the electromagnetic field can take on the form of static electric field equation nabla D=0, that is

$$\frac{\partial D_2}{\partial y} = 0. \qquad (6)$$

The current density of displacement is

$$J = \frac{\partial D}{\partial t}. \qquad (7)$$

Eqs. (1) through (7) constitute the fundamental equations of the piezoelectric effect. In the simultaneous equations (1) through (6), we have the wave motion equation in the following form

$$\rho_m \partial^2 u_1/\partial t^2 = C_{11}^E(1 + e_{21}^2/C_{11}^E \varepsilon_{11}^s)\frac{\partial^2 u_1}{\partial y^2}. \qquad (8)$$

The sine solution of this wave motion equation is

$$u_1 = M \exp[j(\omega_m t - \beta_m y)] + N \exp[j(\omega_m t + \beta_m y)], \qquad (9)$$

omega$_2$ is the resonant frequency; $\beta_m = \omega_m/v_s$ is the acoustic propagation constant of medium; v_s is the speed of sound.

$$v_s = [C_{11}^E/\rho_m(1 + e_{21}^2/C_{11}^E \varepsilon_{11}^s)]^{1/2},$$

M and N are constants to be determined; both constants are related to the boundary conditions. From Eq. (9), in the case of limited thickness of the piezoelectric zone, two terms in the equation should exist simultaneously; that is, the acoustic wave exists in the form of a stationary wave. Considering that all field quantities vary according to $\exp[i\omega_m t]$, the time term can be neglected. Then the oscillation velocity $v_2(y)$ can be written as

$$v_2(y) = j\omega_m[M' \sin \beta_m y + N' \cos \beta_m y]. \qquad (10)$$

Assume that the oscillation velocities (of two thin electrodes) v_1 and v_2 are known, then M' and N' can be determined from the two equations as follows

$$v_1(0) = v_1 = j\omega_m N',$$

$$v_2(d) = -v_2 = j\omega_m [M' \sin\beta_m d + N' \cos\beta_m d]. \qquad (11)$$

From Eq. (7), the displacement current I_2 in the medium can be expressed as

$$I_2 = j\omega_m D_2 A = J_c A, \qquad (12)$$

A is the area of electrode. $j\omega_m D_2$ is the displacement current density in the piezoelectric body. J_c is the density of conduction current in metal electrode. Thus, $D_2 \neq 0$; it is not related to y in the piezoelectric zone. That is

$$D_2 = \text{constant} = I_2/j\omega_m A. \qquad (13)$$

From simultaneous equations (1), (2) and (10) through (13), the electric field distribution and stress distribution in the piezoelectric medium can be obtained as follows.

$$E_2(y) = \frac{1}{\varepsilon_{11}^s}[I_2/j\omega_m A = e_{21}/j(\rho_m/C^D)^{\frac{1}{2}}j\omega_m[M'\cos\beta_m y = N'\sin\beta_m y], \qquad (14)$$

$$T_2(y) = -hJ_2/j\omega_m A + C^D\beta_m/j\omega_m[M'\cos\beta_m d = N'\sin\beta_m d]j\omega_m, \qquad (15)$$

In the above-mentioned equations, constant $h = e_{21}/\varepsilon_{11}^s$ and elasticity coefficient (of piezoelectric medium) $C^D = C_{11}^E(1 + e_{21}^2/C_{11}^E\varepsilon_{11}^s)$ are introduced.

Considering the following conditions in the experiment, the thin sheet resonator is air loading, and the metal electrode layer is infinitely thin (thickness $d' \ll d$), therefore

$$T_2(0) = T_2(d) = 0, \qquad (16)$$

$$v_1 = v_2 = v. \qquad (17)$$

In simultaneous equations (1) through (3) and (14) through (17), the time terms are neglected. By introducing the mechanical electric coupling factor $k^2 = e^2/(C_{11}^E \cdot \varepsilon_{11}^s)$, finally the distributions of electric and acoustic fields in resonator cavity are

$$E_2(y) = j \frac{\ell n v}{v_s \varepsilon_{11} \sin \frac{\ell_m d}{2}} \left\{ [(1 + k^2)/k^2] \cos \frac{\ell_m d}{2} - \cos [\beta_m (d/2 - y)] \right\}, \qquad (18)$$

$$S_2(y) = j \frac{v}{v_s \sin \frac{\ell_m d}{2}} \cos [\beta_m (d/2 - y)]. \qquad (19)$$

Thus. it is apparent that the acoustic wave field (and strain field) in the piezoelectric resonator cavity exists in the form of a stationary wave. The electric field can be divided into two portions: the first term is the homogeneous field with only varying polarization of incident light without producing diffraction effect; the other term is the inhomogeneous portion. The result of the electro-optic effect will lead to an inhomogeneous refraction index in space, thus producing electric grating to cause the incident light to undergo diffraction, and producing the same effect as the acousto-optic grating.

Because of the simultaneous existence of the acousto-optic grating and electro-optic grating in resonant crystals, a coupling effect will certainly occur. This coupling effect can be considered through a simple iterative method. From the photoelastic effect. we know

$$\Delta(1/n^2)_m = P_{m s} S_s \qquad (20)$$

$P_m.$ is photoelastic sensor: S_s is strain. With respect to incident light beam of x polarization, from two equations (19) and (20), the variation of refraction index caused by the acoustic stationary wave is

$$\Delta n_{11} = -\frac{1}{2} n_0^3 P_{11} \frac{v}{v_s \sin \frac{\ell_m d}{2}} \cos [\beta_m (d/2 - y)], \qquad (21)$$

In the equation, n_s is the magnitude of refractive index of incident light in the absence of an electric field and an acoustic field existing in the crystal. Thus, the distribution of the refractive index in the medium caused by the acousto-optic effect is

$$n_s(y) = n_s + \Delta n_{11} = n_s - \frac{1}{2} n_0^3 P_{11} \frac{v}{v_s \sin \frac{\ell_m d}{2}} \cos [\beta_m (d/2 - y)], \qquad (22)$$

6

In the equation, $|\Delta n_{b}/n_{0}| \ll 1$. With consideration, in the meanwhile, given to the portion of inhomogeneous electric field in the second term of the right side, we obtain the following from the primary electro-optic effect

$$\Delta\left(\frac{1}{n^2}\right)_l = r_{li}E_i,\tag{23}$$

r_{li} is the primary electro-optic coefficient of the crystal. Considering that the incident light is in x-polarization, we obtain the following after further differentiation

$$\Delta n_{1E} = \frac{1}{2} r_{11}E_1 n_0^{\prime 3}.\tag{24}$$

Because of the existence of the acousto-optic effect, at this time n_0' is not n_0. First, primary iteration is used; let n_0' approximately equal to $n_0(y)$. Substitute Eq. (22) into the above equation; by retaining the first two terms of the $n_0'(y)$ development equation, we obtain the variation of the refractive index caused by the electro-optic effect

$$\Delta n_{1E} = -\frac{1}{2} n_0^3 r_{11} \frac{e_{11}v}{s_{11}'v_s \sin\dfrac{\beta_m d}{2}} \cos[\beta_m(d/2 - y)]$$

$$+ \frac{3}{8} n_0^5 r_{11} P_{11} \frac{e_{11}v^2}{s_{11}'v_s^2\sin^2\dfrac{\beta_m d}{2}} \cos[2\beta_m(d/2 - y)].\tag{25}$$

At that time, the distribution of the refractive index in the crystal is

$$n_0'' = n_0 + \Delta n_{1S} + \Delta n_{1E}.\tag{26}$$

Considering the second iteration, that is $n_0' = n_0''$. Moreover, applying $\left|\dfrac{\Delta n_{1E}}{n_0}\right| \ll 1$, to again insert Eq. (26) into Eq. (24), thus we obtain the more precise variation of refractive index caused by the electro-optic effect.

$$\Delta n_{1E} = -\frac{1}{2} r_{11} n_0^3 \frac{e_{11}}{s_{11}} \cdot \frac{v}{v_s \sin\dfrac{\beta_m d}{2}} \cos[\beta_m(d/2 - y)]$$

7

$$+ \frac{3}{8} r_{33} \left(P_{13} + r_{33} \frac{e_{33}}{\varepsilon_{11}^s} \right) n_0^3 \frac{e_{33}}{\varepsilon_{11}^s} \frac{v'}{v_s' \sin^3 \frac{\beta_m d}{2}} \cos[2\beta_m(d/2 - y)]$$

$$- \frac{1}{32} r_{33}^2 P_{13} n_0^3 \frac{e_{33}^2}{\varepsilon_{11}^{s2}} \frac{v'}{v_s' \sin^3 \frac{\beta_m d}{2}} \cos[3\beta_m(d/2 - y)]. \tag{27}$$

III. Theoretical Computation and Analysis of Experimental Results

1. From Eq. (27), we can see the following: because of the coupling between the acoustic grating and the electric grating, the result of the primary electro-optic effect leads to the production of the primary grating (i.e., grating constant $\lambda_s = 2\pi/\beta_m$), and production of secondary grating.

$$\left(\lambda_s' = 2\pi/2\beta_m = \frac{1}{2}\lambda_s \right),$$

and tertiary grating $\left(\lambda_s'' = \frac{1}{3}\lambda_s \right),$ that is, the two last terms at the right-hand side of Eq. (27). Comparing Eqs. (27) and (21), the constant of primary grating is the same as the constant of acoustic grating; both constants are $\lambda_s = 2\pi/\beta_m$, . Therefore, the equivalent acoustic grating can be used in the illustration as seen from the following relation.

$$\Delta n_1 = \Delta n_{12} + \Delta n_{13} = -\frac{1}{2} n_0^3 P_{13}' \frac{v}{v_s \sin \frac{\beta_m d}{2}} \cos[\beta_m(d/2 - y)], \tag{28}$$

In the equation, $P_{13}' = P_{13} + r_{33}e_{33}/\varepsilon_{11}^s$ is called the equivalent photoelasticity coefficient. After inserting various parameters of LiNbO$_3$ crystal, we obtain $P_{13}' \approx 0.11$. From readily available texts on piezoelectricity, $P_{13} = 0.072.$ It is apparent that the result of the electro-optic effect resembles increasing the photoelasticity coefficient. This also explains the reason why the diffraction efficiency of the PESO acousto-optic modulator is somewhat due to the acousto-optic effect. Fig. 2 shows a diffraction diagram of He-Ne 6328 Å spectral lines with the PESO acousto-optic modulator (Mg-doped LiNbO$_3$ crystal). In

8

experiments, the ± 11 level is shown but the driving power is only 1 watt, thus accounting for the high diffraction efficiency.
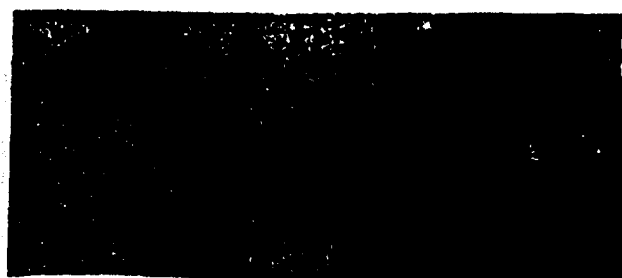

Fig. 2. He-Ne6328Å Raman-Math Diffraction Diagram

$P_{RF} \approx 1W;\ \nu_m = 80MHz$

2. When the driving power is increased, the secondary and tertiary gratings will also have certain function. The secondary grating comes from the coupling of electro-acoustic grating, and also from consideration of the secondary electro-optic effect of the crystal

$$\Delta\left(\frac{1}{n^2}\right)_{ij} = R_{ijkl}E_k E_l, \qquad (29)$$

In the equation, R_{ijkl} is the secondary electro-optic coefficient. After insertion into Eq. (18), the variation of refractive index caused by the secondary electro-optic effect is obtained.

$$\Delta n'_{12} = -\frac{1}{2} n_0^3 R E_3^2$$
$$= A + B\cos[\beta_m(d/2 - y)] + C\cos[2\beta_m(d/2 - y)], \qquad (30)$$

A, B and C are constants not related to coordinate y and time t. We can see that the result of the secondary electro-optic effect is also the production of the secondary grating. From the Raman-Math diffraction angle, we know

$$\sin\theta = m\lambda_0/\lambda_s, \qquad (m = 0,1,2,\cdots), \qquad (31)$$

In the equation, λ_0 is the wavelength of incident light; λ_s is the grating constant. Thus, the diffraction angle of three types of grating can be obtained as follows.

$$\sin \theta = m\lambda_0/\lambda_s, \quad \text{(primary grating)}$$
$$\sin \theta' = 2m\lambda_0/\lambda_s, \quad \text{(secondary grating)}$$
$$\sin \theta'' = 3m\lambda_0/\lambda_s, \quad \text{(tertiary grating)}$$
$$(m = 0,1,2,\cdots). \tag{32}$$

Thus, the first-order diffracted light of the secondary grating is second-order diffracted light of the primary grating. However, the first-order diffracted light of the tertiary grating is the third-order diffracted light of the primary grating. In other words, diffraction light spots emitted from the PESO modulator is the result of superimposing three types of grating diffractions. The spacing of the diffraction spots for the secondary grating is twice the spacing of diffraction spots for the primary grating; it is threefold, in the case of the tertiary grating. The function of the secondary grating is to increase the diffraction energy of the second, fourth, and so on orders; the function of the tertiary grating is to increase the diffraction energy of the third, sixth, and so on orders. Thus, it can be expected that the function of multiple types of gratings will lead to greater relative intensity for the second- and third-order diffracted light over the relative intensity of the second and third-order diffracted light of "pure sound and light" Raman-Math diffraction. Fig. 3 shows a diffraction diagram with a power supply of approximately 2 watts. We can see that result of diffraction for three types of grating is to have very similar light intensities of the three previous orders. Of course, further higher grating orders exist in crystals; this can be obtained from the third iteration to even higher-order iteration; however, their function is much more powerful than the three previous grating orders. Fig. 4 shows an experimental curve of relative intensities of various levels of diffraction light. For easy comparison, the relative intensity curve of various orders of Raman-Math diffraction light for pure acoustic

10

light was plotted, as shown by the dotted curve in Fig. 4. Both curves (solid and dotted curves) have apparent deviation; the solid curve is located higher than dotted curve, thus verifying the above-mentioned conclusion.

$P_{RF} \approx 2W$, He-Ne 6328 Å

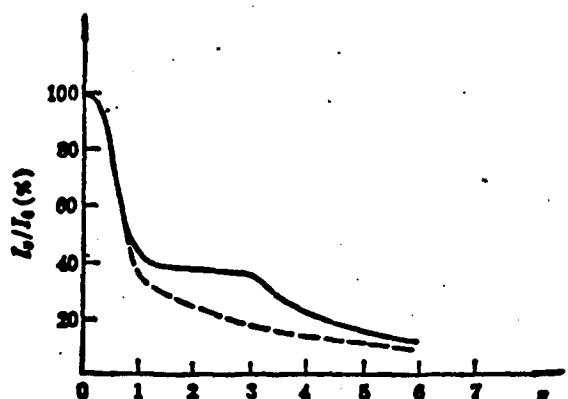Fig. 3.
Diffraction Diagram

$\nu_m \sim 80$ MHz

Fig. 4. Theoretical and Experimental Curves of Relative Intensities of Various Orders Raman-Math Diffracted Light

The paper was received for publication on 24 June 1991.

REFERENCES

[1] L. Turi et al., IEEE. J. Quantum Electron, QE-26 (1990), 1234.
[2] B. A. Auld, Acoustic Fields and Waves in Solids, New York, Wiley-Interscience, (1973).
[3] V. M. Ristic, Principles of Acoustic Devices, New York, Wiley, (1983).

DISTRIBUTION LIST

DISTRIBUTION DIRECT TO RECIPIENT

ORGANIZATION	MICROFICHE
B085 DIA/RTS-2FI	1
C509 BALL0C509 BALLISTIC RES LAB	1
C510 R&T LABS/AVEADCOM	1
C513 ARRADCOM	1
C535 AVRADCOM/TSARCOM	1
C539 TRASANA	1
Q592 FSTC	4
Q619 MSIC REDSTONE	1
Q008 NTIC	1
Q043 AFMIC-IS	1
E051 HQ USAF/INET	1
E404 AEDC/DOF	1
E408 AFWL	1
E410 AFDTC/IN	1
E429 SD/IND	1
P005 DOE/ISA/DDI	1
P050 CIA/OCR/ADD/SD	2
1051 AFIT/LDE	1
P090 NSA/CDB	1
2206 FSL	1

Microfiche Nbr: FTD94C000467L
NAIC-ID(RS)T-0395-94